ELSEVIER

Journal of Alloys and Compounds 296 (2000) 223–228

Journal of ALLOYS AND COMPOUNDS

www.elsevier.com/locate/jallcom

Microstructural and magnetic studies of cast and annealed Nd and PrFeCoBZr alloys and HDDR materials

R.N. Faria[1], B.E. Davies, D.N. Brown, I.R. Harris*

School of Metallurgy and Materials, University of Birmingham, Birmingham, B15 2TT, UK

Received 28 July 1999; accepted 30 July 1999

Abstract

The magnetic properties of HDDR permanent magnets prepared from alloys with a nominal composition of $RE_{13.7}Fe_{63.5}Co_{16.7}B_6Zr_{0.1}$ (RE: Pr and Nd) have been assessed using a permeameter technique. HDDR powders from the alloy in the as-cast and annealed (1100°C for 20 h) conditions were isostatically pressed and bonded in wax before testing. It has been shown that it is possible to produce highly anisotropic HDDR material from the $Pr_{13.7}Fe_{63.5}Co_{16.7}B_6Zr_{0.1}$ alloy in the annealed state, whereas the corresponding $Nd_{13.7}Fe_{63.5}Co_{16.7}B_6Zr_{0.1}$ HDDR material prepared under the same conditions, did not exhibit any significant permanent magnetic properties. The microstructures of both as-cast and annealed alloys have been investigated by scanning electron microscopy and energy dispersive X-ray analysis in an attempt to reveal the reason for this behaviour. Thermomagnetic analysis using in-situ magnetisation measurements have also been carried out on the alloys.

Keywords: Rare earth permanent magnets; HDDR; Microstructure; Anisotropy; Thermomagnetic analysis

1. Introduction

Isotropic and anisotropic hydrogenation disproportionation desorption and recombination (HDDR) powders have been produced with Nd–Fe–B-type materials (see, for example, Refs. [1,2]). Much less effort has been expended on Pr-based HDDR material, but a powder with good remanence but with rather a low coercivity has been reported [3]. Recently, it has also been shown that HDDR powders based on the composition $Pr_{13.7}Fe_{63.5}Co_{16.7}B_6Zr_{0.1}$ could be produced with a high anisotropy and reasonable coercivity after homogenising the alloy and a relatively straightforward, subsequent HDDR treatment [4]. This study also reported that the corresponding $Nd_{13.7}Fe_{63.5}Co_{16.7}B_6Zr_{0.1}$ HDDR powder prepared under the same conditions showed no permanent magnetic properties.

2. Experimental

In this work, the microstructures of these Nd- and Pr-based alloys, both in the as-cast and homogenised conditions, have been studied using a Jeol 6300 scanning electron microscope (SEM). Phase compositions, in terms of elements with atomic numbers >12, were determined using a Link QX2000 energy dispersive X-ray (EDX) spectrometer system fitted to the SEM. The metal compositions of the different phases found in the alloys were determined by EDX on the SEM and were averaged from independent measurements of each phase. The volume relative percentages of each phase in the four microstructures were obtained from image analysis area fractions of optical micrographs, assuming isotropy on a random plane. The morphology of HDDR powders has been investigated by means of a high-resolution Hitachi S-4000 scanning electron microscope (HRSEM).

The alloys investigated in this study were supplied by Rare Earth Products (REP, UK), in the form of slabs (10×10 cm). They had been cast into a 1.5 cm thick rectangular water-cooled copper mould under a vacuum. Subsequent compositional analysis of these as-cast alloys was provided by REP, and are presented in Table 1. Further homogenisation heat treatments to these ingots were carried out under a vacuum (4×10^{-1} mbar) at 1100°C for 20 h. This homogenisation treatment was first employed in NdFeCoBZr alloys [1]. Details of the subsequent HDDR treatment (shown in Fig. 1), the production of permanent magnets from HDDR powders and the

*Corresponding author.

E-mail address: e.b.deer@bham.ac.uk (I.R. Harris)

[1]On leave from the Instituto de Pesquisas Energeticas e Nucleares, IPEN, CNEN, Sao Paulo, Brazil.

0925-8388/00/$ – see front matter
PII: S0925-8388(99)00536-8

Table 1
Chemical analyses of the as-cast alloys (error±0.2wt.%)

Element	Pr-alloy content		Nd-alloy content	
	(at.%)	(wt.%)	(at.%)	(wt.%)
RE	13.5	29.3	13.7	30.0
Fe	63.4	54.5	63.0	53.6
Co	16.9	15.1	17.0	15.3
B	6.1	1.0	6.2	1.0
Zr	0.1	0.1	0.1	0.1

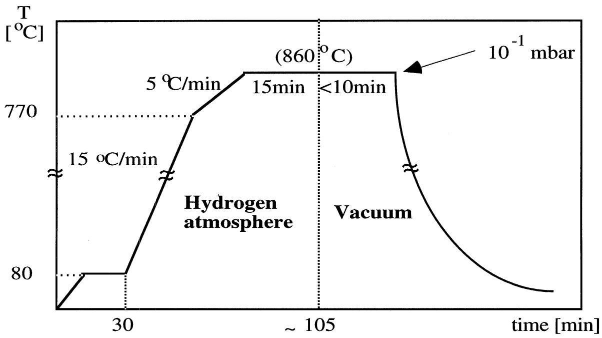

Fig. 1. Schematic diagram of the HDDR treatment cycle.

magnetic measurements have all been given in a previous paper [5]. Following this particular HDDR treatment, the magnetic properties of these alloys were studied using a permeameter. Remanence values have been normalised to assume 100% density of the HDDR sample assuming a linear relationship between density and remanence. A pendulum magnetometer [6] was employed for thermomagnetic analysis (TMA) of the alloys in order to investigate their magnetisation versus temperature behaviour over the temperature range 25–500°C.

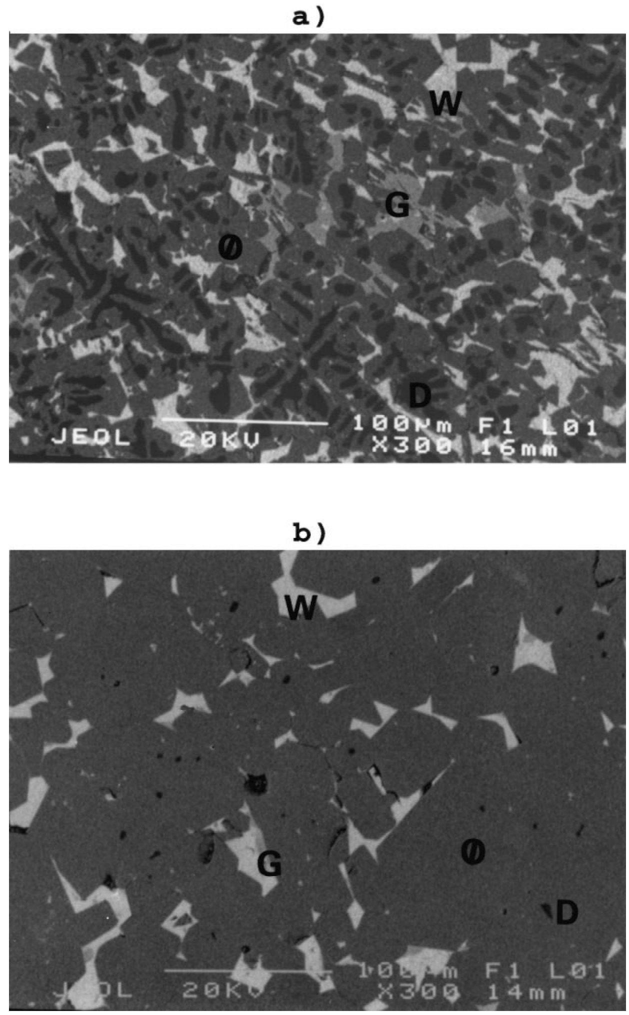

Fig. 2. Backscattered electron image of the $Pr_{13.7}Fe_{63.5}Co_{16.7}B_6Zr_{0.1}$ alloy in the as-cast (a) and annealed condition (b). Table 2 shows the compositions of the Φ, W, G and D phases labeled above.

3. Results

3.1. Microstructural studies

Back-scattered electron images of the as-cast and annealed $Pr_{13.7}Fe_{63.5}Co_{16.7}B_6Zr_{0.1}$ alloy are shown in Figs. 2a and b, respectively. In the as-cast state, this alloy consists of the matrix phase (Φ), a dark dendritic phase (D) within the matrix phase and two phases, grey (G) and white (W) intergranular phases. A comparison between the heat treated structure (Fig. 2b) and the as-cast structure in Fig. 2a indicates the effective removal of the dark phase (D) and some grain growth during the heat treatment. In addition, the grey phase seen at grain boundaries in the as-cast condition is reduced by the heat treatment.

Back-scattered electron images of the as-cast and annealed $Nd_{13.7}Fe_{63.5}Co_{16.7}B_6Zr_{0.1}$ structures are shown in Figs. 3a and b, respectively. As in the previous case with the Pr-based alloy, in the as-cast state, the structure consists of a matrix phase (Φ), a dark dendritic-like phase (D) within the matrix phase and two grain boundary phases, grey (G) and white (W). Again as in the previous case, in the annealed condition (Fig. 3b), the most obvious change from the as-cast condition is the effective removal of the dark phase (D). Further comparison between Figs. 3a and b indicates grain growth following the heat treatment of the alloy. The grey phase in the grain boundaries was also observed in this annealed state. Since the backscattered electron image reveals the difference between the average atomic numbers of the phases, the differences in contrast show that the phases have different compositions.

The phase compositions in these alloys are presented in terms of the ratio RE:Fe:Co:Zr in Table 2. There was a substitution of Co in the matrix phase (Φ) replacing the Fe (Pr:Fe:Co ratio, ~2:10:2.3). No compositional change was observed in the matrix phase as a result of the heat treatment. For both alloys, Fe and Co are observed in the dendritic dark phase (D), which can be attributed to the formation of primary Fe/Co dendrites by the peritectic

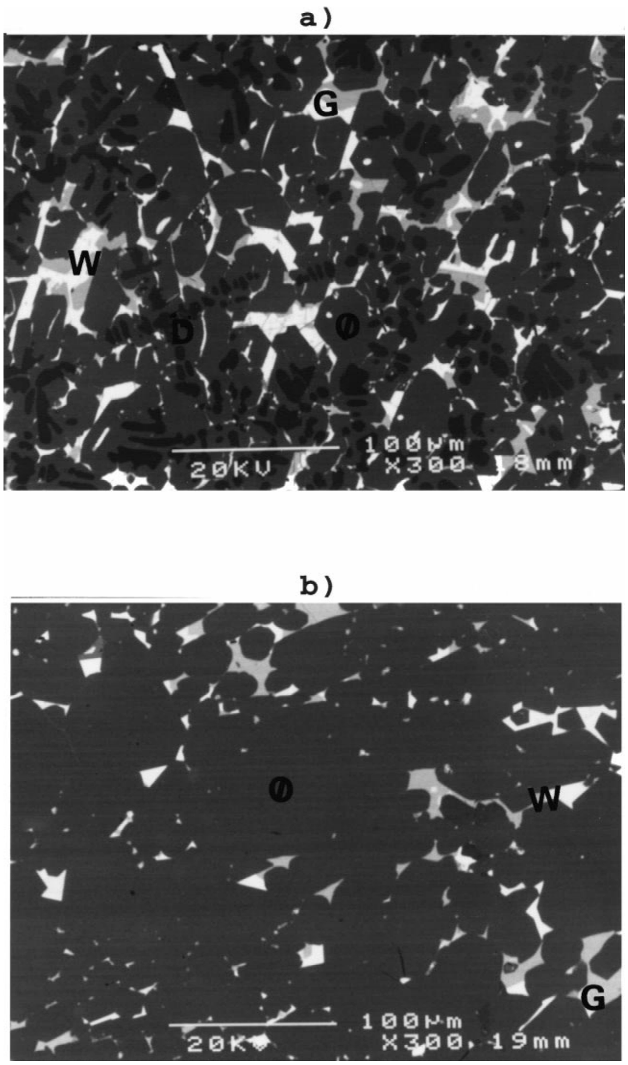

Fig. 3. Backscattered electron image of the $Nd_{13.7}Fe_{63.5}Co_{16.7}B_6Zr_{0.1}$ alloy in the as-cast (a) and annealed condition (b). Table 2 shows the compositions of the Φ, W, G and D phases labeled above.

reactions characteristic of these alloys [7,8]. The white (W) and grey (G) phases have already been identified in previous work [9] as a Nd_3Co phase and $Nd(Fe, Co)_2$ (Laves phase), respectively. The Nd_3Co phase has also been found in the $Nd_{14.4}Dy_{1.6}Fe_{67}V_4B_8$ as-cast alloy and sintered magnet [10]. No evidence of $Nd_{1+\varepsilon}Fe_4B_4$ has been found in the present alloys. The mean area fractions of each of these phases present in the alloys are shown in Table 3. The proportion of changes in phase balances observed with annealing are similar in both alloys, with an increase in the matrix phase at the expense of the other phases.

3.2. Magnetic properties

The magnetic properties of the $Pr_{13.7}Fe_{63.5}Co_{16.7}B_6Zr_{0.1}$ and $Nd_{13.7}Fe_{63.5}Co_{16.7}B_6Zr_{0.1}$ alloys in both as-cast HDDR and annealed HDDR conditions are compared in Table 4. In each case, magnets were prepared from the HDDR powder by the HDDR treatment shown in Fig. 1 and measured using a permeameter [5]. Remanence values have been normalised to assume 100% density of the HDDR sample assuming a linear relationship between density and remanence. Considering both alloys in the as-cast state, the Pr-based alloy shows much better overall magnetic properties. In the annealed condition, a marked improvement in the magnetic properties of the HDDR powder can be seen in the case of the $Pr_{13.7}Fe_{63.5}Co_{16.7}B_6Zr_{0.1}$ alloy. In contrast, the equivalent Nd-based alloy exhibits no hard magnetic properties after this treatment.

Thermomagnetic curves for the Pr- and Nd-based alloys in the annealed condition are presented in Figs. 4 and 5, respectively. As expected, the Curie temperature of the Nd-based alloy is slightly higher than that of the Pr-based alloy. These alloys have a higher Curie temperature in comparison to the conventional Pr–Fe–B materials (290°C) [11] and this can be attributed to the substitution of Co for Fe in the matrix phase. The Curie temperature of the $Nd_2Fe_{14}B$ (310°C) increases linearly with the Co content at about 11°C per at.% [12]. The analysed composition of the Nd-matrix phase gives a Curie temperature

Table 2
Compositions determined by EDX in the hard magnetic matrix phase, the grey phase, the dark phase and the white phase on both alloys (before and after annealing)[a]

Alloy	Phase	RE (at.%)	Fe (at.%)	Co (at.%)	Zr (at.%)
Pr	Φ	14.7±0.7	70.1±0.8	15.2±0.6	<1
As-cast	Grey	38.9±0.9	23.2±0.5	37.9±0.7	<1
Alloy	Dark	<1	88.8±0.9	11.2±0.6	<1
	White	76.3±1.1	<1	23.7±0.6	<1
Pr	Φ	14.5±0.5	69.8±0.6	15.7±0.4	<1
Annealed	White	76.4±0.9	1.2±0.3	22.4±0.4	<1
	Grey	36.2±0.6	25.6±0.5	38.2±0.7	<1
Nd	Φ	14.3±0.7	69.9±0.7	15.8±0.5	<1
As-cast	Grey	42.3±0.9	27.4±0.5	30.3±0.6	<1
Alloy	Dark	<1	88.3±0.8	11.7±0.5	<1
	White	78.5±1.0	<1	21.5±0.5	<1
Nd	Φ	14.2±0.4	69.9±0.4	15.9±0.4	<1
Annealed	White	77.5±0.6	1.7±0.2	20.8±0.3	<1
	Grey	35.4±0.9	33.8±0.5	30.8±0.6	<1

[a] Error bars=±2 standard deviation.

Table 3
Phase balance of the alloy microstructures, presented in terms of percentage area

Phase	Pr-alloy content (%)		Nd-alloy content (%)	
	As-cast	Annealed	As-cast	Annealed
RE-rich	10.9	5.8	6.0	3.7
Φ	54.8	80.0	51.2	85.9
White/Grey	19.0	7.6	12.2	6.3
Dark	15.3	6.6[a]	30.6	4.1[a]

[a] Including porosity and 'pulled-out' areas.

Table 4
Normalised magnetic properties of the Pr- and Nd-based HDDR prepared using the isostatic press technique and measured in the permeameter (error, ±2%)

Alloy	Condition of starting alloy	B_r (mT)	$_iH_c$ (kA/m)	$_bH_c$ (kA/m)	$(BH)_{max}$ (kJ/m)^3)	Sq. (ratio)
$Pr_{13.7}Fe_{63.5}Co_{16.7}B_6Zr_{0.1}$	As-cast	768	487	338	82	0.35
	Annealed	1000	732	548	168	0.49
$Nd_{13.7}Fe_{63.5}Co_{16.7}B_6Zr_{0.1}$	As-cast	504	156	115	16	0.11
	Annealed	–	–	–	–	–

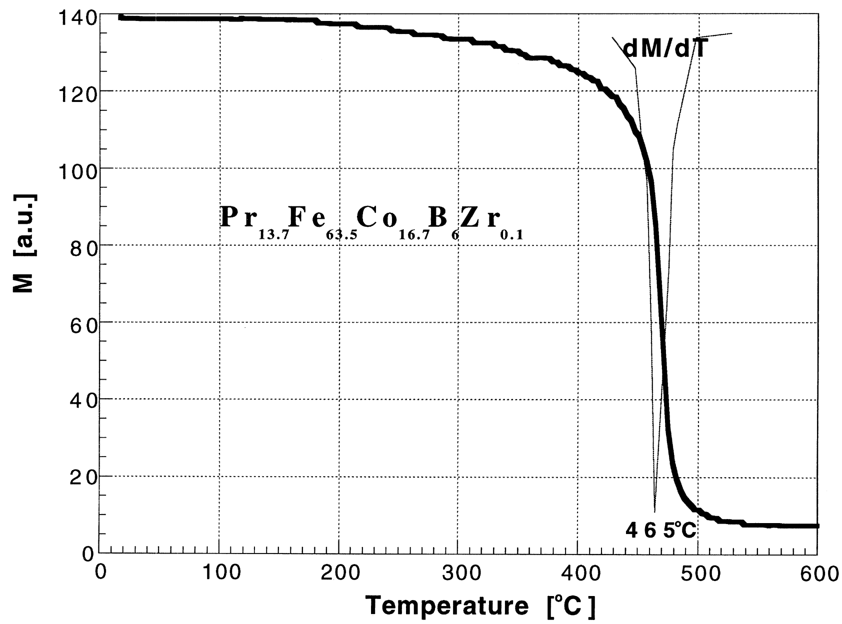

Fig. 4. Magnetisation versus temperature for the $Pr_{13.7}Fe_{63.5}Co_{16.7}B_6Zr_{0.1}$ alloy in the annealed condition.

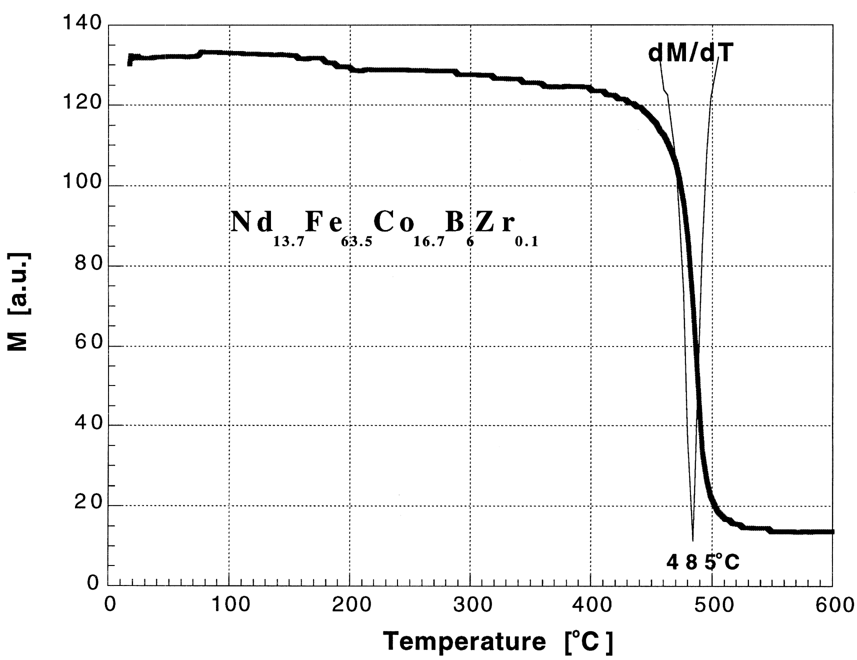

Fig. 5. Magnetisation versus temperature for the $Nd_{137}Fe_{635}Co_{167}B_6Zr_{01}$ alloy in the annealed condition.

of 485°C (310°C+11×15.9°C) in excellent agreement with the present observations (Fig. 5). Assuming an identical dependence of T_c on Co content gives a Curie temperature of 463°C (290°C+11×15.7°C) for the Pr-based alloy, again in excellent agreement with the value shown in Fig. 4.

4. Discussion

It has been reported [8] that, in view of the slower kinetics of formation of the Φ phase in the PrFeB alloys, the annealing of PrFeB magnets must be longer than that of their Nd counterparts. Recently, further evidence that the diffusion rate in PrFeB alloys is rather slower than that of NdFeB alloys under identical conditions, has also been reported [13]. The possibility of a difference in grain growth mechanism between the Pr- and Nd-based alloys, has also been reported for the case of HD sintered magnets [14,15]. Hence, in practical terms, the slower grain growth of Pr-based material, could lead to a greater control of the grain size during and after the recombination stage of the HDDR process. This could lead to improved process flexibility in terms of quenching rate and process duration (as discussed previously [4,5]). The results from the present investigation for the Nd- and Pr-based alloys agrees with the results from previous studies [8,13–15].

The morphology of the HDDR material obtained from the homogenised Nd- and Pr-based alloys using the HDDR treatment shown in Fig. 1 and investigated by means of HRSEM, is shown in Figs. 6a and b. There is a distinctly different morphology for these two powders. The Pr-based material exhibits rounded fine grains, whereas the Nd-based material exhibits a wide range of more facetted grains, more characteristic of a solid/liquid growth mechanism. This difference in grain morphology could be responsible for the radical difference in the magnetic properties of these powders with the facetted grains being more likely to give rise to reverse domain nucleation and hence lower coercivities.

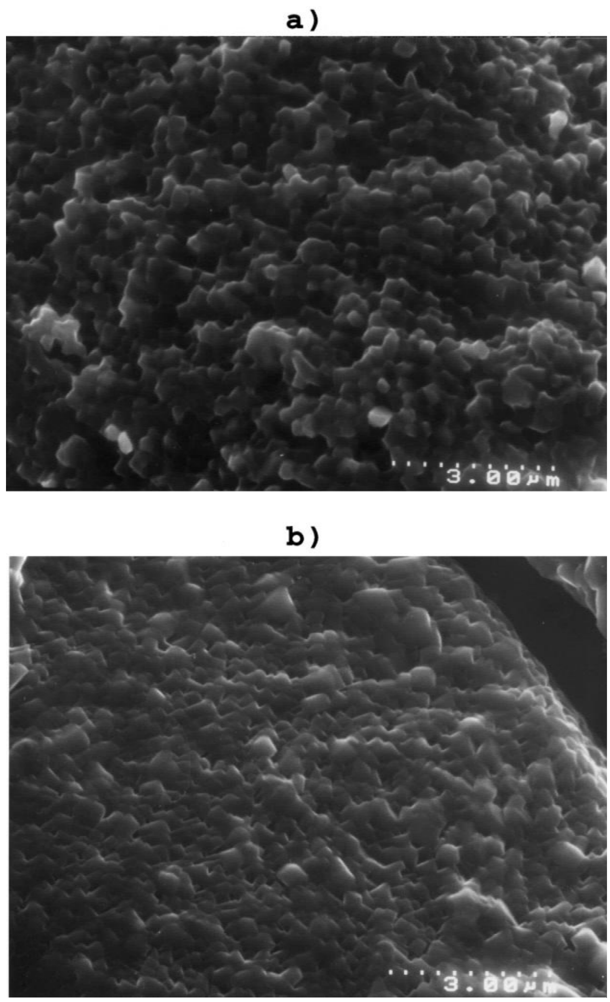

Fig. 6. HRSEM image showing the surface of the $Pr_{13.7}Fe_{63.5}Co_{16.7}B_6Zr_{0.1}$ (a) and $Nd_{13.7}Fe_{63.5}Co_{16.7}B_6Zr_{0.1}$ (b) HDDR material.

5. Conclusions

The present studies show clearly that, using an appropriate processing route, it is possible to produce highly anisotropic magnets using PrFeCoBZr-based HDDR material. A pre-HDDR anneal for 20 h at 1100°C improves significantly the magnetic properties but the same treatment completely eliminates all permanent magnetic properties in the corresponding NdFeCoBZr-based material. This behaviour cannot be explained in terms of compositional changes in the annealing process alone, as the effect on both alloys is very similar, i.e., the removal of the Fe/Co primary dendrites and the corresponding reduction in the amount of RE-rich grain boundary phases. HRSEM studies on the HDDR material indicate that a difference in grain growth and grain morphology could be dominating factors. The smooth, regular grain morphology observed in the case of the Pr-based sample should be more favourable for developing coercivity than the more irregular, facetted structure observed in the corresponding Nd-based material.

Acknowledgements

Many thanks are due to the FAPESP and IPEN-CNEN/SP for the provision of a research grant (R.N. Faria). Thanks are due to REP for the provision of the alloys. Thanks are also due to the EPSRC for the support of the general research programme of which this work forms a part.

References

[1] T. Takeshita, K. Morimoto, J. Appl. Phys. 79 (8) (1996) 5040.

[2] O. Gutfleish, I.R. Harris, in: Fifteenth International Workshop on Rare-Earth Magnets and Their Applications, Dresden, September 1998, 1998, p. 487.

[3] Y.B. Kim, W.Y. Jeung, J. Appl. Phys. 83 (1) (1998) 6405.

[4] R.N. Faria, A.J. Williams, I.R. Harris, J. Alloys Comp. (in press).

[5] R.N. Faria, A.J. Williams, I.R. Harris, J. Magn. Magn. Mater. 202 (1999) 349–353.

[6] C. Burkhardt, F. Dimc, I.R. Harris, J. Magn. Magn. Mater. 157/158 (1996) 127.

[7] Z. Du, D. Wang, W. Zhang, J. Alloys Comp. 284 (1999) 206.

[8] A.C. Neiva, A.P. Tschiptschin, F.P. Missell, J. Alloys Comp. 217 (1995) 273.

[9] J.C.S. Oelli, A.P. Tschiptschin, F.J.G. Landgraf, in: Eighth International Symposium on Magnetic Anisotropy and Coercivity in Rare-Earth Transition Metal Alloys, Birmingham, September 1994, 1994, p. 261.

[10] X.J. Yin, I.P. Jones, I.R. Harris, Magn. Magn. Mater. 116 (1992) L325.

[11] R.N. Faria, X.J. Yin, J.S. Abell, I.R. Harris, Magn. Magn. Mater. 129 (1994) 263.

[12] R.S. Mottram, Ph.D. Thesis, University of Birmingham, 1998, p. 109.

[13] A. Kianvash, I.R. Harris, J. Alloys Comp. 279 (1998) 245.

[14] R.N. Faria, J.S. Abell, I.R. Harris, J. Alloys Comp. 177 (1991) 311.

[15] M.R. Corfield, A.J. Williams, I.R. Harris, in: Fifteenth International Workshop on Rare-Earth Magnets and Their Applications, September 1998, Dresden, 1998, p. 463.